Journal of Alloys and Compounds 509 (2011) 6382–6387

Contents lists available at ScienceDirect

Journal of Alloys and Compounds

journal homepage: www.elsevier.com/locate/jallcom

CuS nanostructures prepared by a hydrothermal method

Qing-Li Huang[a,*], Hu Chen[b], Yong Cai Zhang[b], Chang Le Wu[a]

[a] Testing center, Yangzhou University, Yangzhou city, Jiangsu 225009, China
[b] Key Laboratory of Environmental Material and Environmental Engineering of Jiangsu Province, College of Chemistry and Chemical Engineering, Yangzhou University, Jiangsu 225002, China

ARTICLE INFO

Article history:
Received 2 June 2010
Received in revised form 27 February 2011
Accepted 28 February 2011
Available online 8 March 2011

Keywords:
Chalcogenides
Crystal growth
Copper sulfide
Microstructure

ABSTRACT

Without using any surfactant or template, novel CuS three-dimensional (3D) structures consisting of nanosheets were successfully synthesized via a convenient one-step hydrothermal approach. X-ray diffraction pattern showed that the as-prepared product was pure hexagonal phase CuS. Scanning electron microscopy and high-resolution transmission electron microscopy images revealed that the as-prepared product comprised 3D microspheres (about 1–3 μm in diameter), which were further constructed with randomly oriented, single-crystalline CuS nanosheets (about 20 nm in thickness). The UV–vis absorption spectrum of the as-synthesized CuS 3D microspheres displayed an optical absorption minimum near 672 nm. Besides, the thermal stability of the as-synthesized CuS 3D microspheres was also studied.

1. Introduction

In recent years, materials with three-dimensional (3D) architectures have attracted much attention due to their structural complexities, novel or improved properties, and wide potential applications [1–15]. Among these 3D architectures materials, semiconducting metal sulfides, such as In_2S_3, CdS, SnS, Bi_2S_3, PbS and CuS, have been widely studied, owing to their excellent physical and chemical properties [1–12]. For instance, Liu et al. have prepared 3D flowerlike architectures of β-In_2S_3 assembled with nanoflakes using thiosalicylic acid and carbon disulfide as the double sulfur sources via a one-step solvothermal route [1]. Jiang et al. have synthesized uniform chrysanthemum-like Bi_2S_3 microcrystals assembled from nanosheet building blocks via a convenient hydrothermal synthetic route employing hydrated bismuth nitrate and L-cysteine [2]. Salavati-Niasari et al. have prepared star-shaped PbS nanocrystals using single-source precursor and SnS nanoflowers in the presence of thioglycolic acid via a simple hydrothermal method [8,9].

As one member of the metal sulfides family, CuS is of great interest for materials scientists, owing to its potential applications in catalysts, solar cells and high-capacity cathode materials in lithium secondary batteries, etc. [16–18]. So far, various nanostructures of CuS, including tubular structure [19–21], flower-like morphologies [11,22], urchin-like architecture and snowflake-like pattern [23], plate-like [24], rod-like [25], wire-like [26] and sphere-like [10,27,28] morphologies, etc., have been successfully synthesized via different approaches. However, most of these synthetic methods involved template or complex equipment.

The hydrothermal method provides a promising way for the synthesis of crystalline materials due to its low cost, high efficiency and potential for large-scale production [1–15,19,21,23,24,28]. It not only can induce the formation of well-crystallized products at low temperatures, but also can control the phase, shape and size of the resultant products simply through adjusting the synthesis conditions such as composition of the solution, pH, temperature and duration, etc. Herein, we report a facile hydrothermal route to fabricate CuS 3D microspheres assembled with nanosheets, in the absence of any template and surfactant. The influence of the reaction conditions on the morphology and crystalline structure of the resultant products is investigated. Besides, the optical property and thermal stability of the as-prepared CuS 3D microspheres are also studied.

2. Experimental details

2.1. Material

All the chemical reagents used in this work, including $Cu(NO_3)_2{\cdot}3H_2O$, NH_4F and $(NH_2)_2CS$ are analytically pure.

2.2. Methods

CuS was prepared by using the following procedure: 1.0 mmol of $Cu(NO_3)_2{\cdot}3H_2O$ and 2.0 mmol NH_4F were dissolved in 24 mL of distilled water and the solution was stirred at room temperature for 15 min. Then 6.0 mmol $(NH_2)_2CS$ was added in the

* Corresponding author. Fax: +86 514 87979244.
E-mail address: qlhuang@yzu.edu.cn (Q.-L. Huang).

0925-8388/$ – see front matter © 2011 Elsevier B.V. All rights reserved.
doi:10.1016/j.jallcom.2011.02.167

above solution with stirring. The mixed solution was transferred into a Teflon-lined autoclave of 30 mL capacity. After being sealed and heated at 120 °C for 6 h, the autoclave was cooled to room temperature naturally. The resulting black products were collected by filtration, washed with distilled water and ethanol for several times, and finally dried in air at 70 °C for 6 h.

CuS is known to degrade at temperature above 220 °C in air, it would disproportionate into $(CuS)_x(Cu_2S)_{1-x}$, which will form distinct compounds: $Cu_{1.6}S$, $Cu_{1.8}S$, $Cu_{1.85}S$, $Cu_{1.96}S$, Cu_2S, etc., with significantly different crystal structures. In order to reveal the thermal stability of the as-synthesized CuS 3D structure, this sample was heated in a muffle oven at 200 °C, 300 °C, 400 °C in air for 2 h, respectively.

2.3. Characterization

X-ray diffraction (XRD) patterns were recorded on a Bruker AXSD8 ADVANCE X-ray diffractometer at room temperature. The microstructure analysis was carried out on field emission scanning electron microscopy (FESEM, Hitachi S-4800 field emission scanning electron microscopy), transmission electron microscopy (TEM, FEI Tecnai-12 transmission electron microscopy) and high-resolution transmission electron microscopy (HRTEM, FEI F-30 high-resolution transmission electron microscopy). Raman spectra were measured on a Renishaw Invia Raman spectrometer with a solid-state laser (excitation at 532 nm, 10 mW). Fourier transform infrared spectroscopy (FTIR) spectra were obtained on a Varian FT-IR 7000 spectrophotometer. UV–vis absorption spectra were acquired on a Shimadzu UV-2550 spectrophotometer.

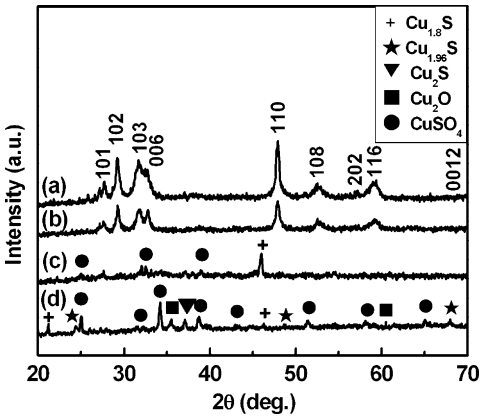

Fig. 1. XRD patterns of (a) the as-prepared CuS 3D microspheres and the residue products after calcinations of the as-prepared CuS 3D microspheres in air at (b) 200 °C, (c) 300 °C and (d) 400 °C for 2 h.

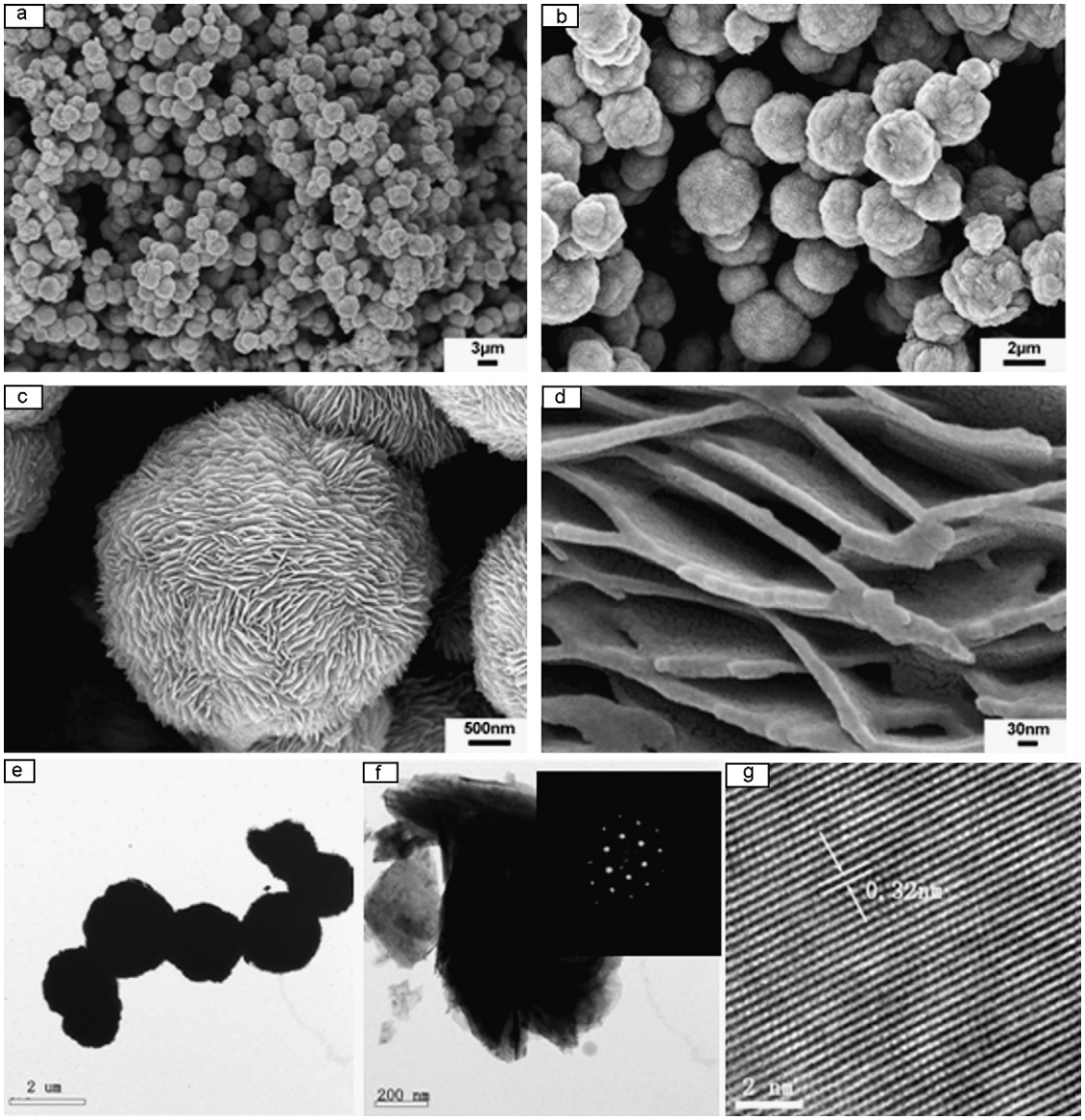

Fig. 2. (a–d) SEM images, (e–f) TEM images and (g) HRTEM image of the CuS 3D microspheres prepared at 120 °C for 6 h (the molar ratio of Cu^{2+} to $(NH_2)_2CS$ was 1:6). The inset image in (f) is the ED pattern performed on the corresponding area.

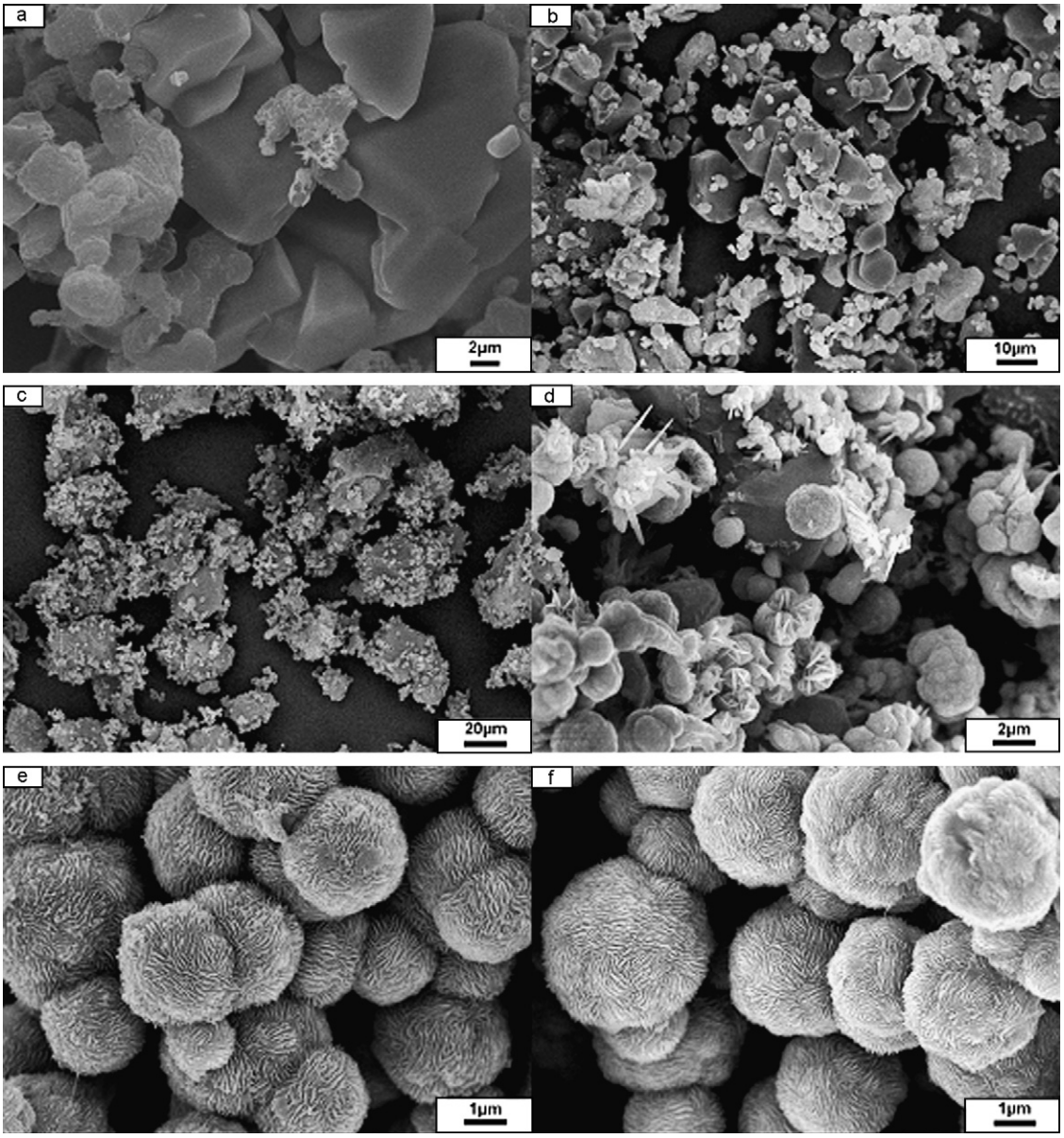

Fig. 3. SEM images of the CuS products prepared at 120 °C for (a) 0 h, (b) 1 h, (c–d) 2 h, (e) 6 h, and (f) 24 h (the molar ratio of Cu^{2+} to $(NH_2)_2CS$ was 1:6).

3. Results and discussion

Fig. 1a shows the XRD pattern of the as-prepared product. All its diffraction peaks can be indexed to hexagonal phase CuS (JCPDS card no. 76-1725, $a = 3.800$ Å, and $c = 16.40$ Å), indicating the successful synthesis of phase-pure CuS powders by the proposed hydrothermal method. Fig. 1b–d shows the XRD patterns of the residue products when the as-synthesized CuS powders were heated in air at 200 °C, 300 °C, 400 °C for 2 h, respectively. As can be seen from Fig. 1b, pure hexagonal phase CuS still remained after heating treatment in air at 200 °C for 2 h. On the other hand, a mixture of $Cu_{1.8}S$ and $CuSO_4$ (Fig. 1c) or $Cu_{1.8}S$, $Cu_{1.96}S$, Cu_2S, Cu_2O, $CuSO_4$ and Cu_2SO_4 (Fig. 1d) was formed, when the heating temperature was increased to 300 or 400 °C, respectively [29].

From the low magnification SEM observation, it can be seen that the as-prepared CuS product comprised many uniform microspheres with diameters ranging from 1 to 3 μm (Fig. 2a). To further examine the microstructure of the microspheres, the higher magnification SEM images were recorded. As shown in Fig. 2b–d, the microspheres were actually composed of numerous 20 nm-thick nanosheets that were randomly arranged to form a dandelion-like structure on the surface of the microspheres. This 3D structure was also confirmed by the TEM images (Fig. 2e and f). The spot-like electron diffraction pattern from a single sheet revealed its single-crystalline nature (inset in Fig. 2f). The HRTEM image of a typical sheet in Fig. 2g showed the clear lattice fringe with a distance of 0.32 nm, agreeing well with the interplanar spacing of (1 0 1) planes of hexagonal phase CuS.

To understand the formation mechanism of the CuS 3D structures, their growth process was followed by examining the products collected at different reaction times. As shown in Fig. 3a, at $t = 0$ h (that is, the electric oven was powered off immediately once the temperature rose from room temperature to 120 °C), the resultant product was totally made up of loosely irregular blocks. When reaction time was prolonged to 1 h, only a few spherical particles formed from the surface of the blocks, as illustrated in Fig. 3b. After reaction for 2 h (Fig. 3c and d), the blocks became fragments and plenty of spherical particles appeared. The blocks decomposed completely and microspheres with rough surface were formed, after reaction for 6 h (Fig. 3e). Further increase of the reaction time

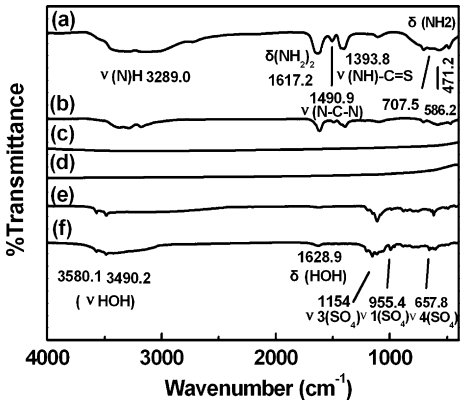

Fig. 4. FTIR spectra of the products prepared at 120 °C for (a) 0 h, (b) 1 h and (c) 6 h (the molar ratio of Cu^{2+} to $(NH_2)_2CS$ was 1:6), and those of the residue products after calcinations of the as-prepared CuS 3D microspheres in air at (d) 200 °C, (e) 300 °C and (f) 400 °C for 2 h.

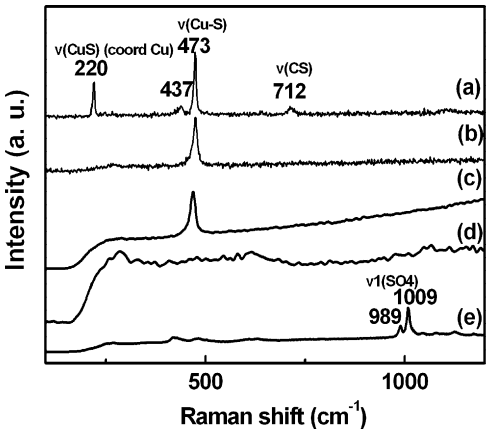

Fig. 5. Raman spectra of the products prepared at 120 °C for (a) 1 and (b) 6 h (the molar ratio of Cu^{2+} to $(NH_2)_2CS$ was 1:6), and those of the residue products after calcinations of the as-prepared CuS 3D microspheres in air at (c) 200 °C, (d) 300 °C and (e) 400 °C for 2 h.

to 24 h, there was little change on the morphology of the product as shown in Fig. 3f.

The FTIR and Raman analysis of the as-prepared products further revealed the detailed evolutionary process. Fig. 4 shows the FTIR spectra of the products obtained at different reaction times. Fig. 4a and b show the FTIR spectra of the products obtained at 0 h and 1 h. The peaks at 3372, 3289, and 3181 cm^{-1} can be assigned to the –NH stretching vibration. The sharp peak at 1617 cm^{-1} can be attributed to $\delta(NH_2)$ vibration. The peaks at 1393 cm^{-1} and 707 cm^{-1} can be assigned to the vibration for the C=S bond and 1490 cm^{-1} due to the C–N stretching vibration. These absorption bands were consistent with the structure of thiourea previously reported [30]. In Fig. 4c, all the absorption bands of thiourea vanished after 6 h of reaction, indicating the formation of pure CuS. Fig. 4d–f shows the FTIR spectra of the residue products when the as-synthesized CuS 3D microspheres were heated in air at 200 °C, 300 °C, 400 °C for 2 h, respectively. The peaks at 1154, 955, and 658 cm^{-1} can be assigned to $\nu_3(SO_4)$, $\nu_1(SO_4)$ and $\nu_4(SO_4)$ mode, respectively. The peaks at 3580 cm^{-1} and 3490 cm^{-1} can be attributed to the mode of ν(HOH) [31,32]. No obvious peaks appeared in Fig. 4d, indicating little change on CuS phase. These results were also consistent with the above XRD analysis.

Fig. 5 shows the Raman spectra of the products obtained at the reaction times of 1 h and 6 h. According to the previous reports [33–35], the peaks at around 220, 439 and 707 cm^{-1} in Fig. 5a were attributed to the structure of thiourea and the coordination condition of Cu^{2+} and thiourea, and the strong peak at 473 cm^{-1} can be assigned to the lattice vibration of CuS [34]. In Fig. 5b, all the Raman peaks of thiourea vanished, further indicating that the transformation process was completed and pure CuS was obtained after 6 h of reaction. The Raman spectra also proved the phase changes of CuS after heating treatment. Fig. 5d–f shows the Raman spectra of the residue products when the as-synthesized CuS 3D structure was heated in air at 200 °C, 300 °C, 400 °C for 2 h, respectively. The only peak at 473 cm^{-1} in Fig. 5d can be assigned to the lattice vibration

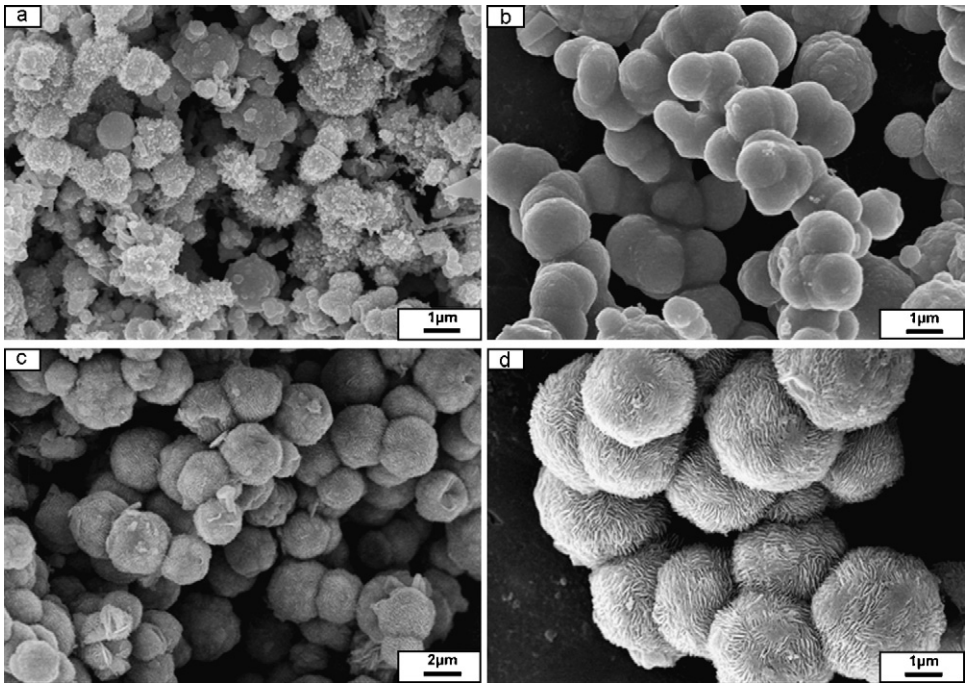

Fig. 6. SEM images of the CuS products prepared at 120 °C for 6 h, with the molar ratios of Cu^{2+} to $(NH_2)_2CS$ being (a) 1:1, (b) 1:3, (c) 1:5 and (d) 1:8.

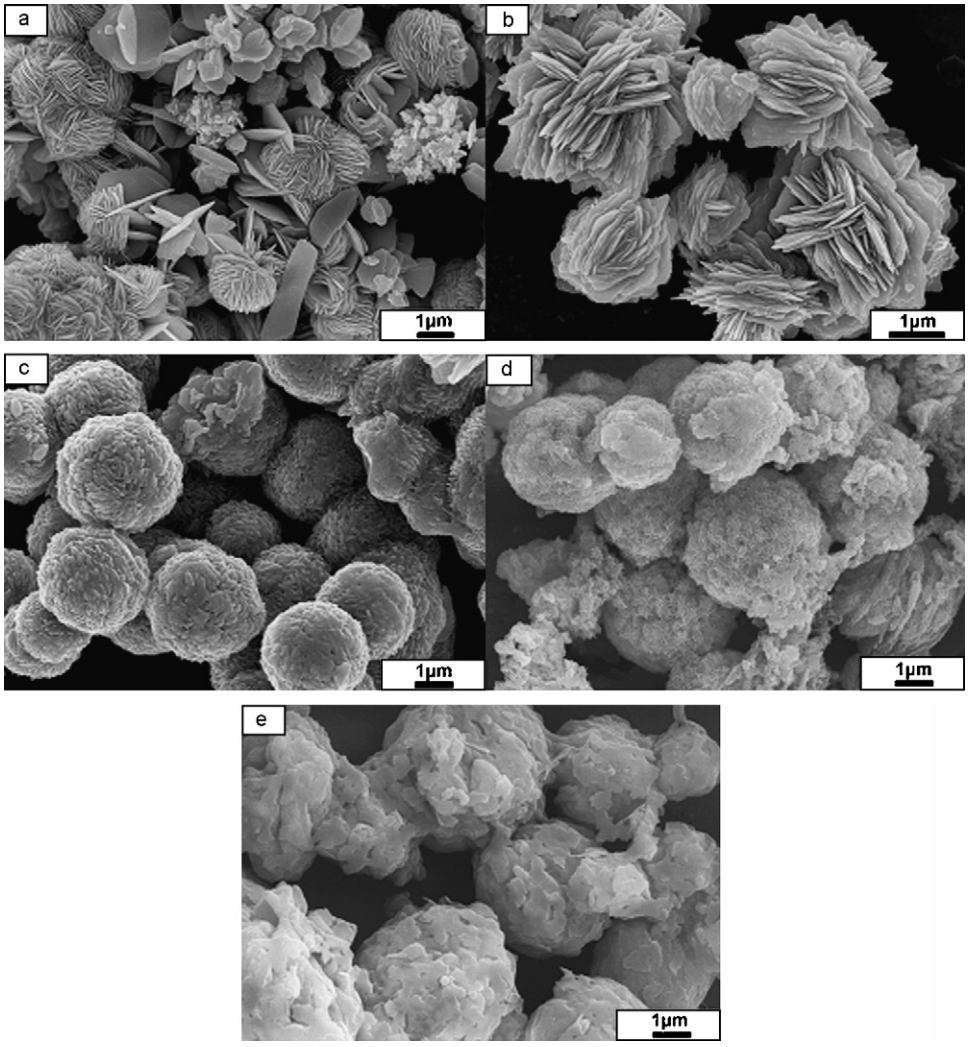

Fig. 7. SEM images of the CuS products prepared at the reaction temperatures of (a) 140 °C and (b) 160 °C (the molar ratio of Cu^{2+} to $(NH_2)_2CS$ was 1:6), and those of the residue products after calcinations of the as-prepared CuS 3D microspheres in air at (c) 200 °C, (d) 300 °C and (e) 400 °C for 2 h.

of CuS, indicating no phase change of CuS after being heated in air at 200 °C for 2 h. No strong peaks in Fig. 5e suggested the decomposition of CuS and poor crystallinity of $Cu_{1.8}S$ and $CuSO_4$. The peaks at around 989 and 1009 cm^{-1} were attributed to the $\nu_1(SO_4)$ mode [31,32].

To further investigate the formation mechanism of the CuS 3D structure, some other experiments were also carried out through varying the reaction conditions such as amounts of $(NH_2)_2CS$ and reaction temperatures. Fig. 6 shows the SEM images of the products obtained using different amounts of $(NH_2)_2CS$ at 120 °C for 6 h. It was evident that the morphologies of the products depended on the amounts of $(NH_2)_2CS$. When 1 mmol $(NH_2)_2CS$ was used, the obtained product had sea urchin and sphere morphologies with diameter ranging from several hundred nanometers to several micrometers (Fig. 6a). When the amount of $(NH_2)_2CS$ was increased to 3 mmol, CuS microspheres with diameter of 1–2 μm were obtained (Fig. 6b), but no nanosheets were found on the surface of the microspheres by detailed observation. However, CuS microspheres consisting of naonsheets were observed when further increasing the amount of $(NH_2)_2CS$ to 5 mmol (Fig. 6c), 6 mmol (Fig. 2) and 8 mmol (Fig. 6d).

In addition, the reaction temperature was also found to play an important role in the microstructures of the products. As shown in Fig. 7a and b, while sphere-like and flower-like structures coexisted in the product synthesized at 140 °C, only flower-like structures were observed in the product synthesized at 160 °C. The different reaction rates at different reaction temperatures were believed to be the main factor affecting the morphologies of the final products. Fig. 7c-e show the SEM images of the residue products when the as-synthesized CuS 3D microspheres were heated in air at 200 °C, 300 °C, 400 °C for 2 h, respectively. The residue products obtained after calcinations can retain the morphologies of their precursor, the as-synthesized CuS 3D structure. But different from the CuS hierarchical structure built up with nanosheets, the surfaces of the residue products after calcinations were gradually collapsed with increasing the heating temperatures (Fig. 7c–e).

According to the above experimental results, the reaction temperature, reaction time and the molar concentration of thiourea all played key roles in the formation of 3D CuS microspheres. Uniform 3D CuS microspheres could be synthesized at 120 °C for reaction times > 6 h and amounts of thiourea > 5 mmol. The formation mechanism of 3D CuS microspheres was thought to be a multistep growth process, involving complexation, decomposition, aggregation, and controlled growth of CuS. In the beginning of hydrothermal process, many complexed CuS clusters consisting of irregular particles were formed, followed by the formation of nucleation clusters. Then, these nucleation clusters decomposed and transformed into CuS nanosheets, which would aggregate to form larger 3D spheres to reduce surface energy. Finally, with further prolonging reaction time to 6 h, these nucleation clusters decom-

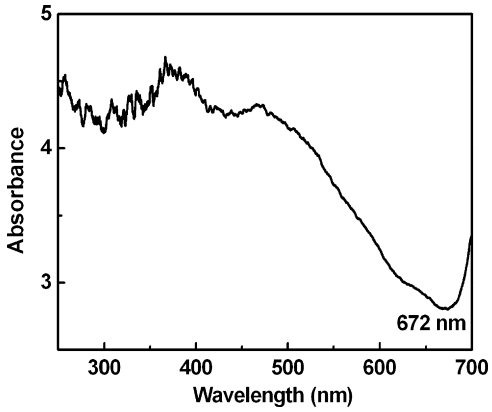

Fig. 8. UV–vis spectrum of the as-prepared CuS 3D microspheres.

pose completely and well-defined 3D CuS nanostructures were formed via Ostwald ripening [36]. This process is similar to the formation process of the flower-like PbS nanostructures synthesized by Salavati-Niasari [8].

CuS is known to be a p-type degenerate semiconductor. The free carrier absorption and high reflection at wavelengths above 700 nm and the onset of band to band absorption at wavelengths below 600 nm bring about an apparent absorption minimum in the 550–750 nm region for this material [37,38]. Fig. 8 shows the UV–vis spectrum of the as-synthesized CuS 3D microspheres. It exhibited an absorption minimum centered at around 672 nm, which was consistent with the reports by Nair et al. [37,38].

4. Conclusions

CuS 3D microspheres were synthesized directly from the hydrothermal reactions of suitable amounts of $Cu(NO_3)_2{\cdot}3H_2O$, NH_4F and $(NH_2)_2CS$ at 120 °C for 6 h. Based on the variation of microstructures of the products with the synthesis conditions including reaction time, reaction temperature and amount of $(NH_2)_2CS$, etc., a plausible "complexation––decomposition––aggregation" mechanism has been proposed. Besides, the optical absorption property and thermal stability of the as-synthesized CuS 3D microspheres were also presented.

Acknowledgements

Thanks to the China Postdoctoral Science Foundation funded project, the Jiangsu Planned Projects for Postdoctoral Research Funds, and the Natural Science Foundation of Jiangsu Province (no. 08KJB150019).

References

[1] L.J. Liu, W.D. Xiang, J.S. Zhong, X.Y. Yang, X.J. Liang, H.T. Liu, W. Cai, J. Alloys Compd. 493 (2010) 309–313.
[2] J.H. Jiang, G.H. Gao, R.N. Yu, G.Z. Qiu, X.H. Liu, Solid State Sci. 13 (2011) 356–360.
[3] Q.F. Han, M.J. Wang, J.W. Zhu, X.D. Wu, L.D. Lu, X. Wang, J. Alloys Compd. 509 (2011) 2180–2185.
[4] J.T. Zai, K.X. Wang, Y.Z. Su, X.F. Qian, J.S. Chen, J. Power Sources 196 (2011) 3650–3654.
[5] L.J. Yao, M.J. Zheng, S.H. He, L. Ma, M. Li, W.Z. Shen, Appl. Surf. Sci. 257 (2011) 2955–2959.
[6] M. Xue, X.H. Zhang, X. Wang, B. Tang, Mater. Lett. 64 (2010) 1357–1360.
[7] C.J. Tang, C.Q. Wang, F.J. Su, C.H. Zang, Y.X. Yang, Z.J. Zong, Y.S. Zhang, Solid State Sci. 12 (2010) 1352–1356.
[8] M. Salavati-Niasari, A. Sobhani, F. Davar, J. Alloys Compd. 507 (2010) 77–83.
[9] M. Salavati-Niasari, D. ghanbari, F. Davar, J. Alloys Compd. 492 (2010) 570–575.
[10] F. Li, J.F. Wu, Q.H. Qin, Z. Li, X.T. Huang, Powder Technol. 198 (2010) 267–274.
[11] J. Liu, D.F. Xue, Mater. Res. Bull. 45 (2010) 309–313.
[12] Z.G. Cheng, S.Z. Wang, D.J. Si, B.Y. Geng, J. Alloys Compd. 492 (2010) L44–49.
[13] R. Chen, Z.R. Shen, H. Wang, H.J. Zhou, Y.P. Liu, D.T. Ding, T.H. Chen, J. Alloys Compd. 509 (2011) 2569–2588.
[14] J.X. Liu, X.L. Dong, X.W. Liu, F. Shi, S. Yin, T. Sato, J. Alloys Compd. 509 (2011) 1482–1488.
[15] Y. Tian, G.M. Hua, W. Xu, N. Li, M. Fang, L.D. Zhang, J. Alloys Compd. 509 (2011) 724–730.
[16] A.E. Raevskaya, A.L. Stroyuk, S.Y. Kuchmii, A.I. Kryukov, J. Mol. Catal. A: Chem. 212 (2004) 259–265.
[17] S.T. Lakshmikvmar, Sol. Energy Mater. Sol. Cell 32 (1994) 7–19.
[18] J.S. Chung, H.J. Sohn, J. Power Sources 108 (2002) 226–231.
[19] T. Thongtem, A. Phuruangrat, S. Thongtem, Mater. Lett. 64 (2010) 136–139.
[20] J.F. Mao, Q. Shu, Y.Q. Wen, H.Y. Yuan, D. Xiao, M.M.F. Choi, Cryst. Growth Des. 9 (2009) 2546–2548.
[21] Y.C. Zhang, T. Qiao, X.Y. Hu, W.D. Zhou, Mater. Res. Bull. 40 (2005) 1696–1704.
[22] C.F. Mu, Q.Z. Yao, X.F. Qu, G.T. Zhou, M.L. Li, S.Q. Fu, Colloids Surf., A: Physicochem. Eng. Aspects 371 (2010) 14–21.
[23] L. Zhu, Y. Xie, X.J. Zheng, J. Cryst. Growth 260 (2004) 494–499.
[24] J. Zhang, Z.K. Zhang, Mater. Lett. 62 (2008) 2279–2281.
[25] P. Roy, K. Mondal, S.K. Srivastava, Cryst. Growth Des. 8 (2008) 1530–1534.
[26] A. Ghahremaninezhad, E. Asselin, D.G. Dixon, Electrochem. Commun. 13 (2011) 12–15.
[27] H.T. Zhu, J.X. Wang, D.X. Wu, Inorg. Chem. 48 (2009) 7099–7104.
[28] M.M. Li, S.Q. Wu, J.L. Shi, J. Alloys Compd. 489 (2010) 343–347.
[29] J.G. Dunn, C. Muzend, Thermochim. Acta 369 (2001) 117–123.
[30] P. Bombicz, I. Mutikainen, M. Krunks, T. Leskela, J. Madarasz, L. Niinisto, Inorg. Chim Acta 357 (2004) 513–525.
[31] V. Hayez, J. Guillaume, A. Hubin, H. Terryn, J. Raman Spectrosc. 35 (2004) 732–738.
[32] M. Bouchard, D.C. Smith, Spectrochim. Acta A 59 (2003) 2247–2266.
[33] B.C. Dave, J.P. Germanas, R.S. Czernuszewicz, J. Am. Chem. Soc. 115 (1993) 12175–12176.
[34] B. Minceva-Sukarova, M. Najdoski, I. Grozdanov, C.J. Chunnilall, J Mol. Struct. 410–411 (1997) 267–270.
[35] R.C. Bott, G.A. Bowmaker, C.A. Davis, G.A. Hope, B.E. Jones, Inorg. Chem. 37 (1998) 651–657.
[36] F.Z. Mou, J.G. Guan, Z.G. Sun, X.A. Fan, G.X. Tong, J. Solid State Chem. 183 (2010) 736–743.
[37] P.K. Nair, V.M. Garcia, A.M. Ferndndez, H.S. Ruiz, M.T.S. Nair, J. Phys. D. Appl. Phys. 24 (1991) 441–449.
[38] M.T.S. Nair, P.K. Nair, Semicond. Sci. Technol. 4 (1989) 191–199.